Pramana – J. Phys. (2018) 90:64
https://doi.org/10.1007/s12043-018-1557-6

Numerical study of entropy generation and melting heat transfer on MHD generalised non-Newtonian fluid (GNF): Application to optimal energy

Z IQBAL, ZAFFAR MEHMOOD and BILAL AHMAD*

Department of Mathematics, HITEC University, Taxila, Pakistan
*Corresponding author. E-mail: bilalahmadgondal@yahoo.com

MS received 6 September 2017; revised 17 November 2017; accepted 23 November 2017; published online 16 April 2018

Abstract. This paper concerns an application to optimal energy by incorporating thermal equilibrium on MHD-generalised non-Newtonian fluid model with melting heat effect. Highly nonlinear system of partial differential equations is simplified to a nonlinear system using boundary layer approach and similarity transformations. Numerical solutions of velocity and temperature profile are obtained by using shooting method. The contribution of entropy generation is appraised on thermal and fluid velocities. Physical features of relevant parameters have been discussed by plotting graphs and tables. Some noteworthy findings are: Prandtl number, power law index and Weissenberg number contribute in lowering mass boundary layer thickness and entropy effect and enlarging thermal boundary layer thickness. However, an increasing mass boundary layer effect is only due to melting heat parameter. Moreover, thermal boundary layers have same trend for all parameters, i.e., temperature enhances with increase in values of significant parameters. Similarly, Hartman and Weissenberg numbers enhance Bejan number.

Keywords. Tangent hyperbolic fluid; numerical solutions; melting heat transfer; entropy generation; optimal energy.

PACS Nos **44.25.+f; 47.10.ad; 47.50.−d**

1. Introduction

It is well known that some fluids do not adhere to classical Newtonian viscosity description. These are classified as non-Newtonian fluids. One special class of fluids is of considerable practical importance in the field of science and technology. In these fluids, viscosity depends on shear stress or flow rate. Moreover, viscosity of most non-Newtonian fluids, such as polymers, is usually a nonlinear decreasing function of generalised shear rate. This is known as shear-thinning behaviour. Tangent hyperbolic fluid model exhibits rheological characteristics of such fluids (Ai and Vafai [1]). The tangent hyperbolic fluid is used extensively for different laboratory experiments. Friedman *et al* [2] used tangent hyperbolic fluid model for large-scale magneto-rheological fluid damper coils.

The study of boundary layer flows over a stretching sheet has been considerably increased because of their tremendous applications in different fields of science and engineering. Some of the examples include hot rolling, continuous stretching, aerodynamic extrusion of plastic sheets, polymer industries etc. Revolutionary study in this context was conducted by Sakaidis [3]. Crane [4] and Gupta and Gupta [5] have analysed continuous moving surface problem with constant surface temperature. Many contributions to this problem including stretching velocity and study of heat transfer are available in literature (see [6,7]).

The first analysis on induced magnetic field was done by Vishnyakov and Pavlov [8]. In their analysis, viscous fluids have been considered. Theory of magnetohydrodynamics (MHD) concerns with inducing current in a moving conductive fluid in the presence of magnetic field, which creates force on electrons of conductive fluid and also changes magnetic field itself. A survey of MHD studies can be found in [9]. Singh and Gupta [10] have discussed MHD-free convective flow of a viscous fluid through a porous medium bounded by an oscillating porous plate in slip flow regime with mass transfer.

In thermodynamics, the measure of disorder is called entropy. According to the second law of thermodynamics for an isolated system, system spontaneously grows toward thermodynamic equilibrium and attains minimum entropy. On the other hand, for a non-isolated system, there is a possibility of a decrease in entropy of a system, which may transfer the same amount of entropy to surroundings. Heat transfer and viscous dissipation play vital roles in changing the behaviour of entropy of a system. Study of entropy generation is a field of interest among researchers. Different sources such as heat transfer and viscous dissipation are responsible for the generation of entropy [11,12]. Bejan [13] investigated entropy generation rate in a circular duct with forced heat flux at the boundary and its extension to determine optimum Reynolds number as a function of Prandtl number. Sahin [14] introduced second law analysis to a viscous fluid in circular duct with isothermal boundary conditions. Falahat [15] discussed entropy generation of nanofluids in helical tube and laminar flow. In another paper, Sahin [16] presented the effect of variable viscosity on entropy generation rate for a heated circular duct. In more recent papers, Mahmud and Fraser [17,18] used second law analysis to convective heat transfer problems and to non-Newtonian fluid flow between two parallel plates. Saouli and Saouli [19] studied entropy generation in a liquid film falling along an inclined heated plate. Some recent articles for readers' interest are cited in refs [20,21].

For any engineering system, an optimal and efficient system is desired. In order to examine the efficiency of the system, one has to study the facts contributing to energy loss. In thermodynamics, this energy loss is measured by measuring the entropy generation and irreversibility ratio. These two parameters play vital roles to analyse the process through which engineering system attains its thermal equilibrium. The present entropy generation analysis is carried out for melting heat transfer of MHD GNF model. Moreover, conducting equations of two-dimensional tangent hyperbolic fluid are modelled. With the help of dimensionless parameters, entropy generation analysis is discussed numerically with the assistance of the shooting method.

2. Problem development

Assume a steady incompressible flow of a tangent hyperbolic fluid over a stretching sheet situated at the initial line, i.e. on x-axis ($y = 0$). Consider that the fluid is under the influence of a magnetic field of strength B_0 that is applied in positive y-direction normal to the plate. Moreover, melting at a steady rate is incorporated with constant property. The x- and y-axes are taken along and perpendicular to the sheet, respectively, and the flow is being confined to the region $y \geq 0$. The velocity of stretching sheet is considered to be $u_w(x) = ax$, where a is a positive stretching sheet constant. The temperature of the melting surface T_m and ambient temperature T_∞ have been chosen such that $T_\infty > T_m$. The induced magnetic field due to magnetic Reynolds number is taken to be small enough and negligible when compared to the applied magnetic field. Physical flow situation is presented in figure 1.

The governing equations of the boundary layer flow, heat and mass transfer of a tangent hyperbolic fluid are [22]:

$$\frac{\partial u}{\partial x} + \frac{\partial v}{\partial y} = 0, \tag{1}$$

$$u\frac{\partial u}{\partial x} + v\frac{\partial u}{\partial y} = \nu\,(1-n)\,\frac{\partial^2 u}{\partial y^2} + \sqrt{2}\nu n\Gamma\left(\frac{\partial u}{\partial x}\frac{\partial^2 u}{\partial y^2}\right) - \frac{\sigma B_0^2}{\rho}u, \tag{2}$$

$$u\frac{\partial T}{\partial x} + v\frac{\partial T}{\partial y} = \frac{k}{\rho C_p}\frac{\partial^2 T}{\partial y^2}, \tag{3}$$

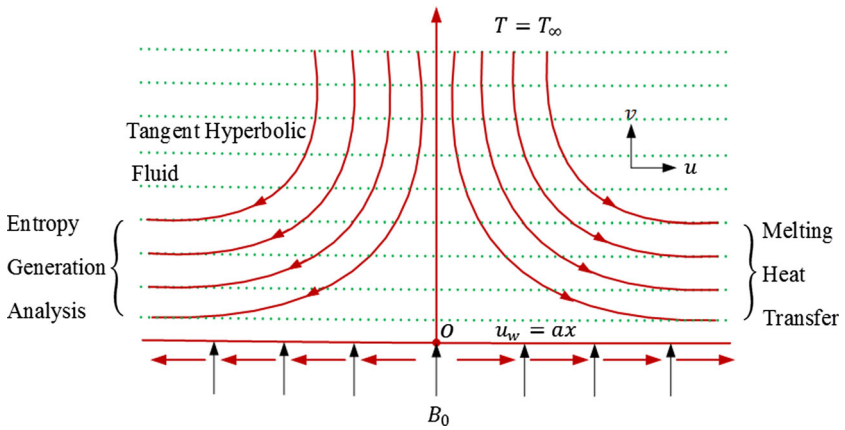

Figure 1. Engineering flow structure.

where u and v are velocity components in x- and y-directions, respectively. n is the behaviour index. It represents Newtonian behaviour of fluid for $n = 1$, shear thinning when $n > 1$ and shear thickening when $n < 1$. T is the fluid temperature, C_p is the specific heat, k is the thermal conductivity, ρ is the fluid density, $\nu = \mu/\rho$ (ratio of viscosity to density of fluid) is the kinematic viscosity. The associated boundary conditions are

$$u = u_w(x) = ax, \quad v = 0, \quad T = T_w \ \text{ at } y = 0,$$
$$u \to 0, \quad \frac{\partial u}{\partial y} \to 0, \quad T \to T_\infty \ \text{ as } y \to \infty, \tag{4}$$

with

$$k\left(\frac{\partial T}{\partial y}\right)\Big|_{y=0} = \rho\left[\lambda + c_s(T_m - T_0)\right] v(x, 0). \tag{5}$$

In the above equations, λ is the latent heat of fluid and c_s is the heat capacity of the solid surface. The boundary conditions defined in eq. (4) explain that the heat conducted to the melting surface is equal to the heat of melting plus sensible heat required in rising solid temperature T_0 to its melting temperature T_m. The boundary layer equations (1)–(3) admit solution of the form:

$$u = axf'(\eta), \quad v = \sqrt{a\nu}\, f(\eta), \quad \eta = \sqrt{\frac{a}{\nu}}\, y,$$
$$\theta(\eta) = \frac{T - T_w}{T_\infty - T_w}. \tag{6}$$

Equation (1) is automatically satisfied, and (2)–(3) become

$$(1-n)f''' + ff'' - (f'')^2 + nW_e f'' f''' - M^2 f' = 0, \tag{7}$$
$$\theta'' + \Pr f\theta' = 0 \tag{8}$$

and the corresponding boundary conditions (4) are

$$f'(0) = 1, \quad \theta(0) = 0, \quad \Pr f(0) + M_1\theta'(0) = 0,$$
$$f'' \to 0, \quad \theta \to 1 \text{ as } \eta \to \infty, \tag{9}$$

where primes denote differentiation with respect to η, Pr is the Prandtl number, Weissenberg number, W_e is the fluid parameter, M is the Hartman number and M_1 is the dimensionless melting parameter. It is a combination of Stefan numbers $c_f(T_\infty - T_w)/\lambda$ and $c_s(T_w - T_0)/\lambda$ for liquid and solid phases, respectively. Mathematically, we have

$$W_e = \sqrt{\frac{2a}{\nu}}\, ax\Gamma, \quad \Pr = \frac{k}{\rho C_p},$$
$$M_1 = \frac{c_f(T_\infty - T_w)}{\lambda + c_s(T_w - T_0)},$$
$$M^2 = \frac{\sigma B_0^2}{\rho a}. \tag{10}$$

The skin friction coefficient C_f and local Nusselt number Nu_x are

$$C_f = \frac{\tau_w}{\rho u_w^2},$$
$$\mathrm{Nu}_x = \frac{xq_w}{k(T_\infty - T_w)}, \tag{11}$$

in which expressions of wall skin friction (τ_w) and wall heat flux (q_w) are given by

$$\tau_w = (1-n)\frac{\partial u}{\partial y} + \frac{n\Gamma}{\sqrt{2}}\frac{\partial^2 u}{\partial y^2}\Big|_{y=0},$$
$$q_w = -\left(k + \frac{16\sigma^* T_\infty^3}{3k^*}\right)\frac{\partial T}{\partial y}\Big|_{y=0}. \tag{12}$$

With the help of dimensionless variables (10), we have

$$C_f\,(\mathrm{Re}_x)^{-1/2} = (1-n)f''(\eta) + \frac{n}{2}W_e\left(f''(\eta)\right)^2\Big|_{\eta=0},$$
$$\mathrm{Nu}_x \mathrm{Re}_x^{-1/2} = -\theta'(0), \tag{13}$$

where $\mathrm{Re}_x = ax^2/\nu$ is the local Reynolds number.

3. Entropy generation analysis

The following expression indicates entropy generation:

$$E_G = \frac{k}{T_\infty}\left[\left(\frac{\partial T}{\partial x}\right)^2 + \left(\frac{\partial T}{\partial y}\right)^2\right] + \tau L. \tag{14}$$

Entropy generation due to fluid friction is a non-dimensional quantity denoted as N_s. It is the ratio of actual entropy generation rate E_G to characteristic entropy transfer rate E_{G_0} and is given as

$$E_{G_0} = \frac{k\Delta T}{l^2 T_\infty^2}, \quad \Lambda = \frac{\Delta T}{T_\infty}, \tag{15}$$
$$N_s = \frac{E_G}{E_{G_0}} = \left(\frac{\partial T}{\partial y}\right)^2 + \frac{\gamma}{\Lambda}\left(\frac{\partial u}{\partial n}\right)^2. \tag{16}$$

In eq. (16), first term on the right side represented as N_h is entropy due to heat transfer and second one is due to viscous dissipation termed as N_f, i.e.,

$$N_s = N_h + N_f. \tag{17}$$

Ratio between entropy generation due to fluid friction and Joule dissipation to total entropy generation due to heat transfer is known as irreversibility ratio. It is defined as

$$r = \frac{N_f}{N_h} = \frac{(\gamma/\Lambda)\,(\partial u/\partial n)^2}{(\partial T/\partial y)^2}. \tag{18}$$

It is worth mentioning that heat transfer irreversibility dominates in the region $0 \le r < 1$ and fluid friction with

magnetic effects dominates when $r > 1$. Moreover, heat transfer and combined effect of friction and magnetic field is in equilibrium when $r = 1$. Another irreversibility parameter is Bejan number B_e. It is defined as

$$B_e = \frac{1}{1+r}. \tag{19}$$

It has a range from 0 to 1. The combined effect of fluid friction and magnetic field is prominent when $B_e \to 0$. For $B_e \to 1$, it is the case for entropy generation due to the dominant effect of heat transfer irreversibility. Equilibrium occurs when $B_e = 1/2$, i.e., when entropy generation crops up due to the same effects of heat transfer and fluid friction.

4. Computational procedure

The solution of eqs (7)–(8) along with boundary conditions (9) is computed by employing a numerical technique known as shooting method. Here, we convert nonlinear equations into a system of five first-order ordinary differential equations by labelling variables as $f = y_1$, $f' = y_1' = y_2$, $f'' = y_2' = y_3$, $\theta = y_4$, $\theta' = y_4' = y_5$. This yields the following mathematical expressions:

$$\begin{pmatrix} y_1' \\ y_2' \\ y_3' \\ y_4' \\ y_5' \end{pmatrix} = \begin{pmatrix} y_2 \\ y_3 \\ \dfrac{1}{1-n+nW_e y_2^2}(y_3^2 + M^2 y^2 - y^1 y^3) \\ y_5 \\ -\Pr\, y_1 y_5 \end{pmatrix},$$

$$\begin{pmatrix} y_1(0) \\ y_2(0) \\ y_3(0) \\ y_4(0) \\ y_5(0) \end{pmatrix} = \begin{pmatrix} \dfrac{-M_1\theta'(0)}{\Pr} \\ 1 \\ f''(0) \\ 0 \\ \theta'(0) \end{pmatrix}.$$

Then, we solve it by Runge–Kutta method of order 5. The iterative process will be terminated when error involved is $< 10^{-6}$.

5. Description of results

The flow and heat transfer in tangent hyperbolic fluid has been solved numerically using shooting method. The expressions of velocity and temperature have been used to compute entropy generation and Bejan number. Figures 2–6 depict the effects of various material parameters, such as Prandtl number Pr, melting parameter M_1, Weissenberg number W_e and magnetic parameter M, on velocity profile $f'(\eta)$. Figure 2 shows that an increase in W_e decreases the boundary layer thickness because the fluid parameter causes a resistance in the velocity of fluid, i.e. fluid velocity is remarkably affected by this physical parameter. For the case of shear thinning fluids, fluid parameter plays a role in increasing fluid flow which leads to a decrease in boundary layer thickness. Same trend can be seen for power law index n and Prandtl number Pr (see figures 3 and 4). It is depicted that Pr contributes in lowering the velocity profile. The influence of melting parameter M_1 on velocity profile is illustrated in figure 5. It causes an increase in boundary layer thickness. Figure 6 shows the influence of increasing magnetic parameter M. It decreases the fluid velocity leading to an enhanced boundary layer thickness. Figures 7–10 describe the impact of several physical numbers on temperature profile $\theta(\eta)$. In figure 7, it can be observed that W_e influences in enhancing temperature. The temperature profile has similar behaviour in comparison to other parameters like n, M_1 and magnetic parameter M.

Figures 11–13 show the effects of parameters on skin friction coefficient and local Nusselt number. The effect of Weissenberg number W_e on skin friction is seen in figure 11. It explains that skin friction is an increasing function of applied magnetic field and opposite trend is seen against W_e. Moreover, from figure 12, it is depicted that skin friction decreases by rising power law index.

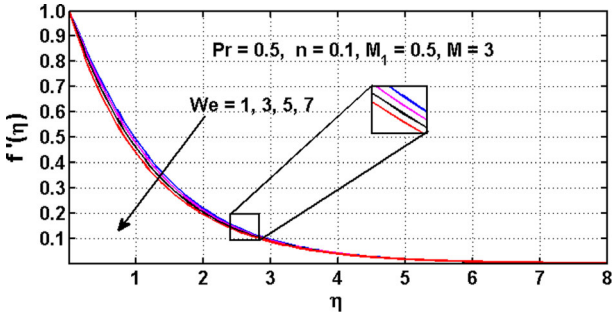

Figure 2. Impact of W_e on $f'(\eta)$.

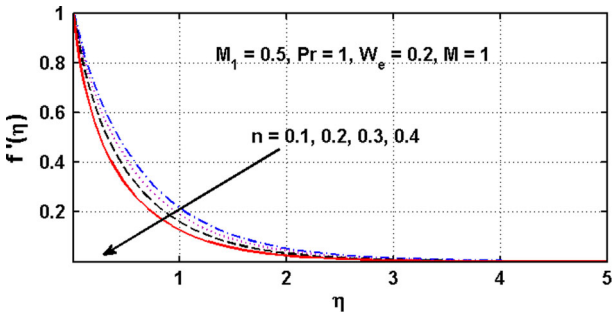

Figure 3. Variation of n on $f'(\eta)$.

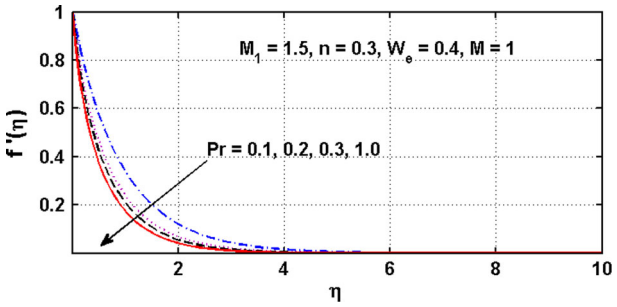

Figure 4. Behaviour of Pr on $f'(\eta)$.

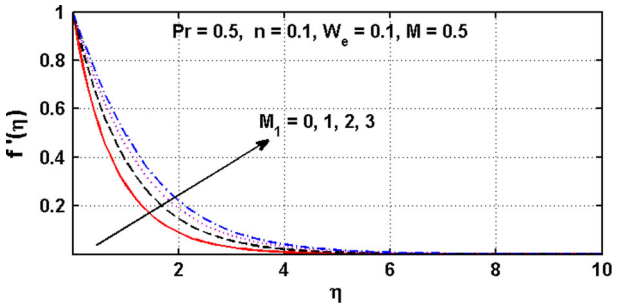

Figure 5. Impact of M_1 on $f'(\eta)$.

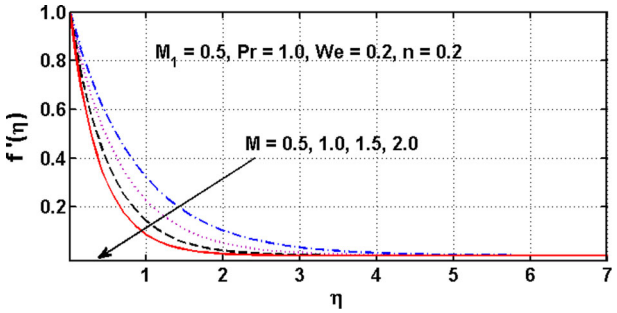

Figure 6. Influence of M on $f'(\eta)$.

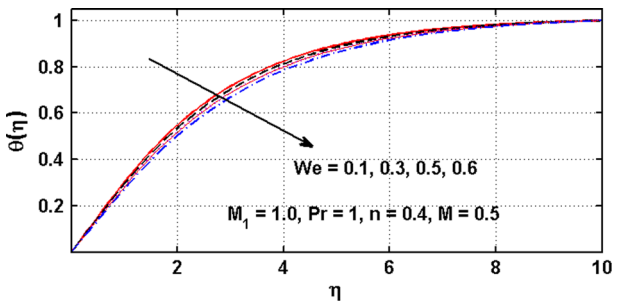

Figure 7. Effect of W_e on $\theta(\eta)$.

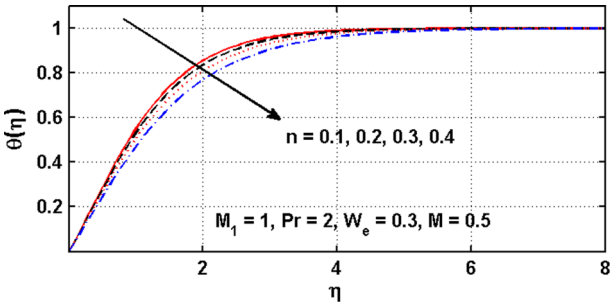

Figure 8. Impact of n on $\theta(\eta)$.

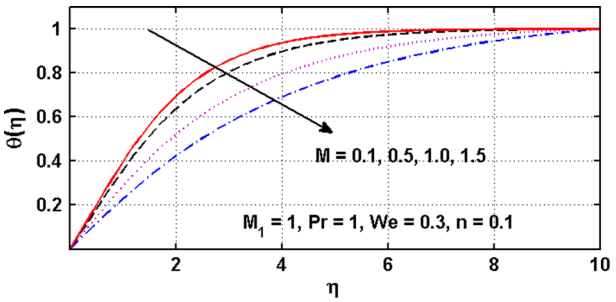

Figure 9. Behaviour of M on $\theta(\eta)$.

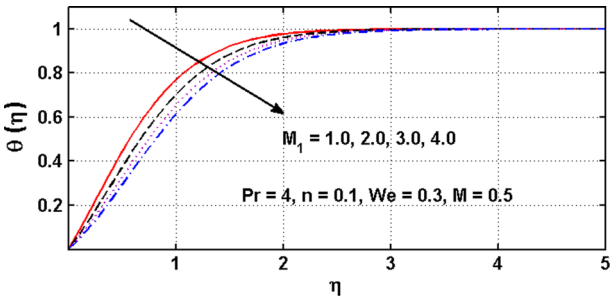

Figure 10. Influence of M_1 on $\theta(\eta)$.

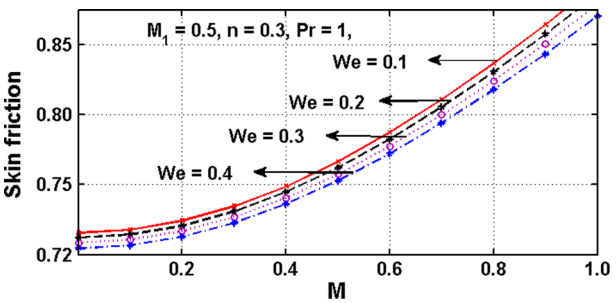

Figure 11. Variation of W_e on $(\mathrm{Re}_x)^{1/2}C_f$ against M.

Figure 13 shows the effect of power law index on Nusselt number when plotted against applied magnetic field. It can be seen that both M and n play roles in decreasing Nusselt number.

5.1 *Analysis of thermal equilibrium*

N_s and B_e are the two significant non-dimensional parameters in entropy generation analysis. Entropy

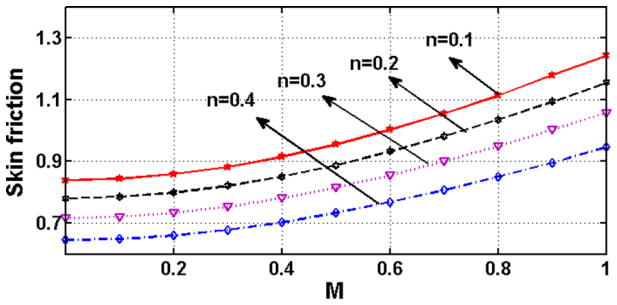

Figure 12. Effect of n on $(\mathrm{Re}_x)^{1/2}C_f$ against M.

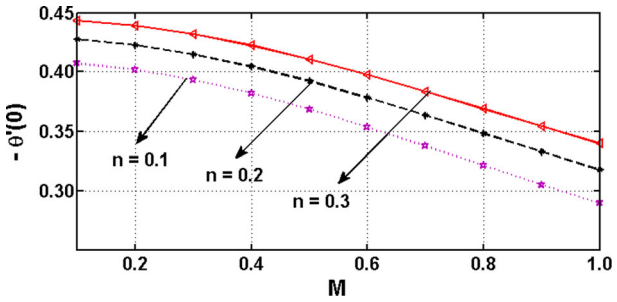

Figure 13. Variation of n on $(\mathrm{Re}_x)^{1/2}\mathrm{Nu}_x$ against M.

generation number N_s consists of two major factors, N_h (due to heat transfer) and N_f (due to viscous dissipation). Graphical illustrations of entropy generation and Bejan numbers can be seen in figures 14–19. Figures 14–16 demonstrate the effect of power law index, applied magnetic field and fluid parameter on N_s. It is depicted that the parameters n and W_e contribute in decreasing N_s due to the fact that, more shear thinning behaviour of fluid has more energy loss. However, the applied magnetic field, being a resistance force, contributes in up-surging it. Effects of pertinent parameters n, M and W_e on irreversibility parameter are displayed in figures 17–19. Analysis of these graphs concludes that all the three significant parameters contribute in enlarging Bejan number. $B_e \to 1$ is significant in the sense that it shows the dominant role of viscous dissipation. It is observed that viscous dissipation gets dominant where boundary layer ends.

Further, table 1 gives values of Nusselt number for different influential parameters. From this table, we noticed that Nusselt number increases with an increase in Hartman, Weissenberg and index numbers. Table 2 represents the behaviour of entropy number N_s, entropy due to heat generation N_h and entropy due to viscous dissipation N_f with respect to significant parameters. It is clear from the table that Pr is related directly with N_h, N_s and N_f and inversely related to index n, Weissenberg number W_e, Hartman number M and dimensionless parameter Λ.

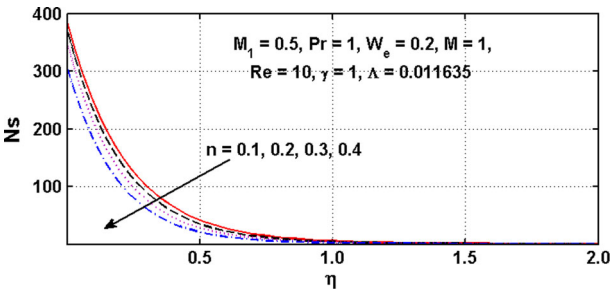

Figure 14. Result of power index n on N_s.

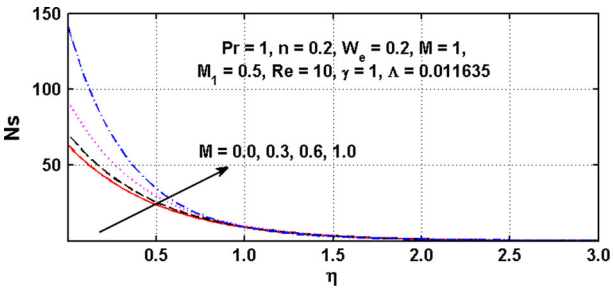

Figure 15. Outcome of M on N_s.

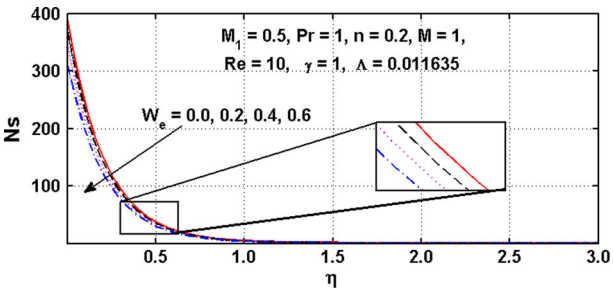

Figure 16. Influence of W_e on N_s.

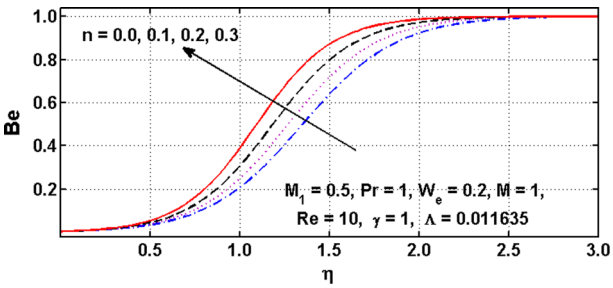

Figure 17. Effect of power index n on B_e.

6. Summary

The present analysis explained boundary layer flow of hyperbolic tangent fluid with combined effects of MHD and melting heat transfer. The main findings of the present analysis are:

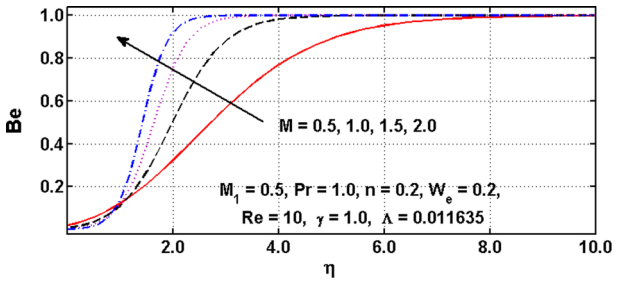

Figure 18. Variation of M on B_e.

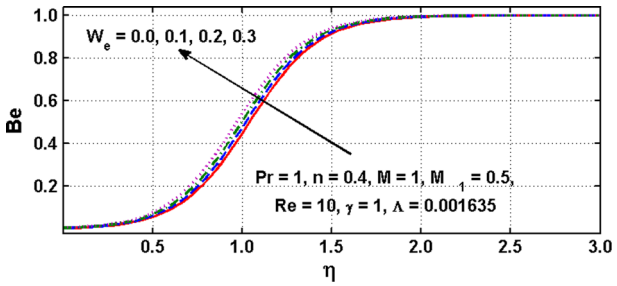

Figure 19. Impact of W_e on B_e.

- The rate of transport reduces with increase in Prandtl number Pr and hence viscous boundary layer diminishes.

Table 1. Numerical results analysis of $-\theta'(0)$ for physical parameters n, M and W_e.

n	M	W_e	Nusselt number: $-\theta'(0)$
0.0	0.0	0.1	0.8939
0.1			0.9386
0.2			0.9912
0.3	0.5		1.2026
	1.0		1.5734
	1.5		2.0559
	0.5	0.3	1.2678
		0.5	1.3240

- The effect of index n, Weissenberg W_e and Hartman M numbers on viscous and thermal boundary layers is the same.
- Velocity and temperature profile decrease with an increase in magnetic, index and Weissenberg numbers.
- Results of M, n and W_e are the same for entropy generation number, but reverse in the case of Bejan number.
- Melting parameter contributes in lessening the entropy of flow.
- There is an increase in skin friction coefficient when n and W_e increase.
- Influence of n and W_e on B_e and N_s is quite opposite.
- Thermal equilibrium is attained within the boundary layer.

Table 2. Computational analysis for entropy generation.

Pr	n	W_e	M	M_1	Re	γ	Λ	N_h	N_f	N_s
1.0	0.2	0.2	2.0	0.5	10	1.0	0.011635	0.8197	380.6602	381.4799
2.0								2.0872	386.2029	388.2901
3.0								3.8770	388.2227	392.0996
4.0	0.3							4.7933	319.5442	324.3374
	0.4							5.4674	367.7308	373.1983
	0.5							3.8331	157.9181	161.7512
	0.1	3.0						6.4241	398.0315	404.4556
		4.0						6.3907	393.6704	400.0611
		5.0						6.3565	389.0455	395.4020
		2.0	1.0					4.3451	825.3465	829.6916
			1.5					3.0083	1.411×10^3	1.414×10^3
			2.0					2.2013	2.160×10^3	2.160×10^3
			0.5	20				4.1680	394.5991	398.7671
				30				2.9339	386.9139	389.8478
				40				2.1920	381.3081	383.5001
				10	1.5			12.9773	406.0613	419.0386
					2.0			19.4659	406.0613	425.5272
					2.5			25.9545	406.0613	432.0159
					1.0	0.5		25.9545	609.0920	635.0465
						1.0		25.9545	812.1227	838.0772
						1.5		25.9545	1.015×10^3	1.041×10^3
						1.5	0.5	25.9545	9.4490	35.4036
							1.0	25.9545	4.7245	30.6790

- Dominant effects of viscous dissipation exist at free stream.

References

[1] L Ai and K Vafai, *Num. Heat Transfer* **47**, 955 (2005)
[2] A J Friedman, S J Dyke and B M Phillips, *Smart Mater. Struct.* **22**, 045001 (2013)
[3] B C Sakiadis, *AIChE J.* **7**, 26 (1961)
[4] L J Crane, *Z. Angew. Math. Phys.* **21**, 645 (1970)
[5] P S Gupta and A S Gupta, *Can. J. Chem. Engg.* **55**, 744 (1977)
[6] T Hayat, Z Abbas and M Sajid, *Chaos Solitons Fractals* **29**, 840 (2009)
[7] S Nadeem, A Hussain and M Khan, *Commun. Non-Linear Sci. Numer. Simulat.* **15**, 475 (2010)
[8] V I Vishnyakov and K B Pavlov, *Magnetohydrodynamics* **8**, 174 (1972)
[9] R Moreau, *Magnetohydrodynamics* (Kluwer Academic Publishers, Dordrecht, 1990)
[10] P Singh and C B Gupta, *Indian J. Theor. Phys.* **53**, 111 (2005)
[11] A Bejan, *Adv. Heat Transfer* **15**, 1 (1982)
[12] A Bejan, *J. Appl. Phys.* **79**, 1191 (1996)
[13] A Bejan, *J. Heat Transfer* **101**, 718 (1979)
[14] A Z Sahin, *J. Heat Transfer* **120**, 76 (1998)
[15] A Falahat, *IJMSE* **2**, 44 (2011)
[16] A Z Sahin, *Heat Mass Transfer* **35**, 499 (1999)
[17] S Mahmud and R A Fraser, *Int. J. Therm. Sci.* **42**, 177 (2003)
[18] S Mahmud and R A Fraser, *Exergy* **2**, 140 (2002)
[19] S Saouli and S A Saouli, *Int. Comm. Heat Mass Transfer* **31**, 879 (2004)
[20] N C Peddisetty, *Pramana – J. Phys.* **87**: 62 (2016)
[21] M M Bhatti, A Zeeshan and R Ellahi, *Pramana – J. Phys.* **89**: 48 (2017)
[22] N S Akbar, S Nadeem, R Ul Haq and Z H Khan, *Indian J. Phys.* **87**, 1121 (2013)